Chemistry–A European Journal
Research Article
doi.org/10.1002/chem.202200404
Chemistry Europe
European Chemical Societies Publishing
www.chemeurj.org

Synthesis of Intramolecular P/Al-Based Frustrated Lewis Pairs via Aluminum-Tin-Exchange and their Reactivity toward CO_2

Patrick Federmann,[a] Robert Müller,[b] Fabian Beckmann,[a] Caroline Lau,[a] Beatrice Cula,[a] Martin Kaupp,*[b] and Christian Limberg*[a]

Dedicated to Prof. Holger Braunschweig on occasion of his 60th birthday.

Abstract: Frustrated Lewis pairs (FLPs) composed of acidic alane and basic phosphane functions, separated by a xanthene linker, can be prepared through the corresponding Me_3Sn derivative and methyl aluminum compounds with elimination of Me_4Sn. This way MeClAl-, Cl_2Al- and $(C_6F_5)_2Al$-moieties could be introduced and the resulting FLPs are stabilized by a further equivalent of the alane precursors. In contact with the FLPs CO_2 is bound via the C atom at the phosphane functions and the two O atoms at the Al centers. The residues at the latter determine the binding strength. Hence, in case of MeClAl CO_2 capture occurs at higher pressure and under ambient conditions CO_2 is released again, while for Cl_2Al and $(C_6F_5)_2Al$ CO_2 binding becomes irreversible. The results of DFT calculations rationalize these findings by the high thermodynamic stabilization in case of more electronegative residues, which concomitantly lead to higher barriers, and in case of $(C_6F_5)_2Al$ further stabilization is achieved through a low reorganization energy.

Introduction

Intramolecular frustrated Lewis pairs (FLP) based on Lewis acidic boron centers have been extensively studied in recent years.[1] Representatives bearing an aluminum acceptor site, however, remain rare due to synthetic challenges that are associated with its high intrinsic Lewis acidity and the fragility of the Al–C bond.[2] So far, merely two synthetic strategies[3] to connect an Al^{III} center with the carbon atom of an organic linker scaffold have been followed, namely hydroalumination[4] and transmetalation from organolithium compounds[2,5] (Scheme 1). Both perform well for close arrangements of Lewis acid and base such as geminal and vicinal patterns, but are only conditionally suitable for bringing the components into a larger spatial separation.

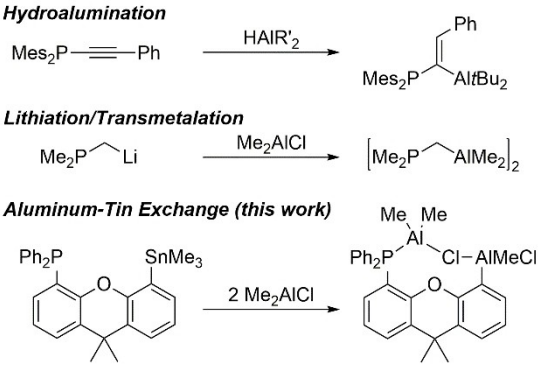

Scheme 1. Synthetic approaches to form P/Al-based frustrated Lewis pairs.

Our initial endeavors to synthesize an intramolecular P/Al-based FLP on a xanthene backbone by lithiation and transmetalation resulted in the irreversible coordination of the utilized solvent (Et_2O, THF) to the Lewis acidic Al^{III} center. This led to interesting insights with regard to the functioning of such FLPs, exemplarily for the ring-opening of THF,[6] but further applications were limited: the solvents are bound tightly and cannot be replaced by external substrates, so that the Lewis acid site is quenched. Consequently, we sought to develop an alternative route that leads to the corresponding solvent-free xanthene-linked Al/P FLP. Obviously, on such a route the aluminum-carbon bond linking the Al site to the xanthene

[a] P. Federmann, F. Beckmann, C. Lau, Dr. B. Cula, Prof. Dr. C. Limberg
Institut für Chemie
Humboldt-Universität zu Berlin
Brook-Taylor-Straße 2, 12489 Berlin (Germany)
E-mail: christian.limberg@chemie.hu-berlin.de
[b] Dr. R. Müller, Prof. Dr. M. Kaupp
Institut für Chemie
Theoretische Chemie/Quantenchemie, Sekr. C7
Technische Universität Berlin
Straße des 17. Juni 135, 10623 Berlin (Germany)
E-mail: martin.kaupp@tu-berlin.de

Supporting information for this article is available on the WWW under https://doi.org/10.1002/chem.202200404

backbone has to be established in non-coordinating solvents to allow for subsequent reactivity toward small molecules.

Eisch et al. and Gabbaï et al. independently reported on the exchange of trimethylstannyl groups bound to *sp*- or sp^2-hybridized carbon atoms by alkylaluminum chlorides in aliphatic or aromatic solvents (Scheme 2).[7] However, these two unique examples did not allow for conclusions as to whether the presence of a Lewis base (e.g. a xanthene-bound diphenylphosphine moiety) might adversely affect the desired transmetalation. Beckmann et al. reported on the attempted synthesis of diphenylphosphinoacenaphthylaluminum dichloride starting from the corresponding tri-*n*-butylstannyl precursor and aluminum trichloride, but no conversion could be observed.[5g] Contrarily, the other group 13 E^{III} trichlorides (E = B, Ga, In, Tl) did show reactivity, suggesting that a phosphine function does not generally act as an inhibitor. Herein, we present our findings on the applicability of aluminum-tin transmetalations in the synthesis of a xanthene-linked Al/P-based FLP and the utilization of the generated systems for CO_2 activation.

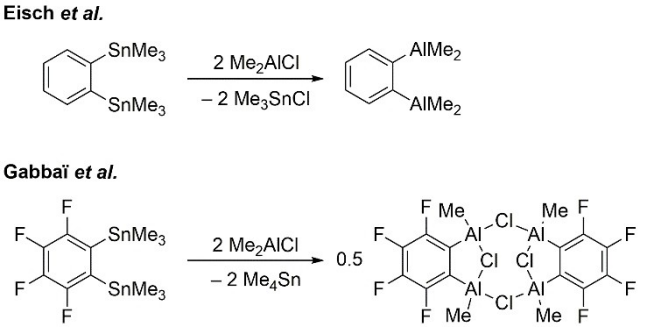

Scheme 2. Aluminum-tin exchange under formation of different by-products as reported independently by Eisch et al. and Gabbaï et al.

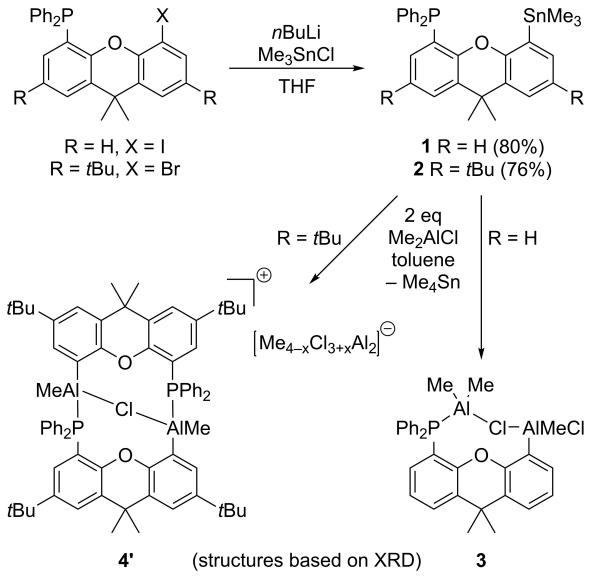

Scheme 3. Synthetic routes to FLPs **3** and **4** via aluminum-tin exchange starting from the corresponding stannanes **1** and **2**.

Results and Discussion

The starting materials for our studies 4-trimethylstannyl-5-diphenylphosphino-9,9-dimethylxanthene **1** and 4-trimethylstannyl-5-diphenylphosphino-2,7-di-*tert*-butyl-9,9-dimethylxanthene **2** were synthesized from the respective 4-iodo and 4-bromo precursors.[8] Lithiation in THF and subsequent addition of trimethyltin chloride yielded in **1** and **2**, which could be isolated in good yields of 80% and 76%, respectively (Scheme 3). Both compounds were fully characterized by ^{1}H, ^{13}C, ^{31}P and ^{119}Sn NMR spectroscopy, single crystal XRD and elemental analysis. It is noteworthy, that the ^{1}H NMR spectra of **1** and **2** in C_6D_6 exhibit prominent signals at $\delta = -0.47$ ppm and $\delta = -0.50$ ppm, respectively, which originate from the trimethylstannyl moiety, distinctive due to their ^{119}Sn and ^{117}Sn satellites.

With these starting materials in hand, the Al–Sn exchange was addressed. While Gabbaï et al. had observed a Me–Al/Sn–C metathesis to produce Me_4Sn, Eisch et al. reported a Cl–Al/Sn–C metathesis yielding in Me_3SnCl as the by-product of the exchange. Therefore, dimethylaluminum chloride was selected as the reagent, as this enabled the system to react via any of the two types of pathways. Treatment of **1** and **2**, respectively, with one equivalent of Me_2AlCl in C_6D_6 led to the slow formation of a new species as indicated by ^{31}P and ^{1}H NMR spectroscopy. In the ^{31}P NMR spectra this new product resonates at a chemical shift of $\delta = -16.7$ ppm for the conversion of **1** and of $\delta = -16.3$ ppm for the conversion of **2**, respectively. Both ^{1}H NMR spectra featured an intense signal at $\delta = 0.00$ ppm regardless of the chosen xanthene precursor, which was thus attributed to the by-product. The chemical shift of this resonance in combination with its integral suggests Me_4Sn as secondary product and therefore a reactivity resembling the one reported by Gabbaï and coworkers.

However, unlike in case of the reported examples, the conversion stopped at 50% even after heating the reaction mixture to 80 °C for several hours indicating a 1:2 stoichiometry of the transformation. Indeed, when two equivalents of Me_2AlCl were added, the precursors **1** and **2**, respectively, as judged by NMR spectroscopy, were fully consumed and selectively converted into single products, which as outlined below were identified as ^{H}Xant(PPh_2–$AlMe_2Cl$–AlMeCl), **3**, and ^{tBu}Xant(PPh_2–$AlMe_2Cl$–AlMeCl), **4**. The high selectivity of the reactions allowed for simple workup by evaporating the solvents and Me_4Sn to give **3** and **4** quantitatively in satisfactory purity (Scheme 3). Both compounds are sensitive toward air and moisture and degrade slowly at room temperature to multiple unidentified species.

Attempts to grow single crystals of **3** and **4** suitable for X-ray diffraction analysis were performed by slow diffusion of *n*-hexane into saturated solutions of the compounds in toluene. The molecular structures determined for the resulting crystals are shown in Figure 1. Interestingly, quite different solid state structures were found in spite of the close resemblance of the precursors **1** and **2**. In both cases, the anticipated formation of an Al–C bond at the xanthene scaffold has been achieved successfully and the concomitant elimination of Me_4Sn, as

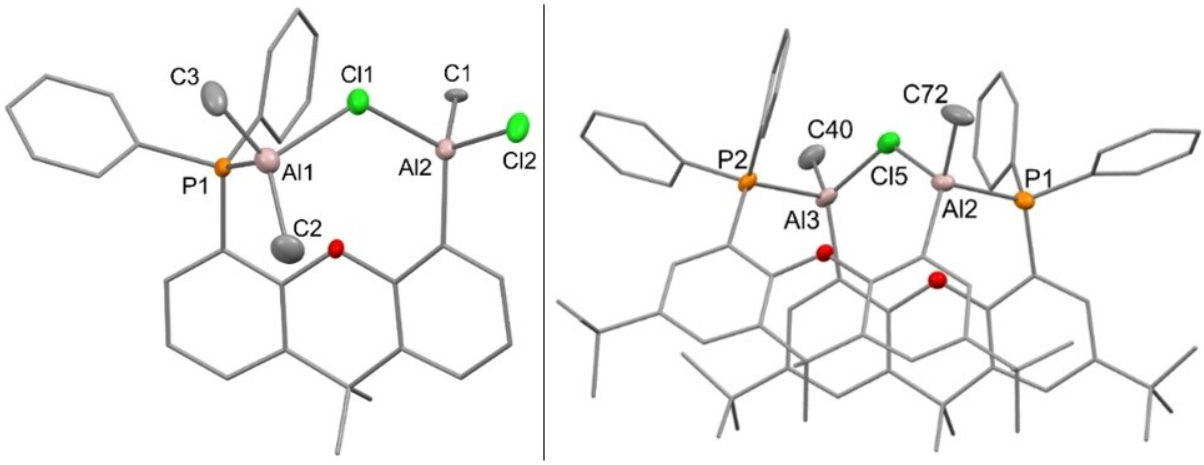

Figure 1. Molecular structures of one independent molecule of the asymmetric unit of **3** (left) and the complex cation of **4′** (right) as determined by X-ray diffraction analysis. H atoms omitted for clarity; thermal ellipsoids drawn at the 50% probability level. Due to disorder isotropic refinement was conducted on the phenyl and *tert*-butyl groups of the cation and the methyl and chloride groups in the anion in **4′**. Selected bond lengths (Å) and angles (°): (for **3**) P1-Al1 2.467(3), Al1-C2 1.957(7), Al1-C3 1.924(8), Al1-Cl1 2.252(2), Al2-Cl1 2.301(2), Al2-Cl2 2.162(3), Al2-C1 1.971(5), P1-Al1-Cl1 99.15(9), Al1-Cl1-Al2 120.1(1); (for **4′**) P1-Al2 2.474(2), P2-Al3 2.471(2), Al2-Cl5 2.237(2), Al3-Cl5 2.250(2), Al2-C72 .1.952(5), Al3-C40 1.951(7), P1-Al2-Cl5 95.95(7), P2-Al3-Cl5 95.17(7), Al2-Cl5-Al3 118.79(8). The structural parameters of the four independent molecules of the asymmetric unit of **3** are nearly identical; slight deviations are noted for the Al–Cl–Al bridge for which the bond lengths measure between 2.240–2.264 Å and 2.295–2.314 Å, respectively.

inferred from the ^{1}H NMR spectra, is further confirmed, as the Al-center bound to the xanthene is surrounded by one methyl and one chlorido group. The structure of **3** is monomeric and charge-neutral as the second equivalent of Me_2AlCl that was required to reach full conversion is bound in an FLP type fashion in-between the Lewis basic phosphine and the Lewis acidic xanthene-bound alane sites. By contrast, the structure determined for crystals grown from solutions of **4**, corresponding to a salt **4′**, can be rationalized as follows: Two xanthene molecules, each equipped with a Ph_2P and an Al(Me)Cl unit, have dimerized via intermolecular mutual contacts between the acid and base sites. One of the chloride ligands from the resulting molecule has been abstracted by two equivalents of the Me_2AlCl precursor leading to the anion $[Me_4Cl_3Al_2]^-$ (the latter is disordered in the crystal, containing varying ratios of Me/Cl). The remaining chlorido ligand in the corresponding cation thus formed enters a bridging position between both aluminum centers.

While the solid state structure of **3** rationalizes that a second equivalent of Me_2AlCl is required, the structure of **4′** does not, as the additional alane molecule is not incorporated in the FLP entity but rather acts as chloride scavenger and thus is not recognizably needed for a full conversion of the precursor **2**. Therefore, the structure found for **4′** may well not correspond to the primary product of the reaction but might form only during the crystallization process. This hypothesis is underpinned by the occurrence of a single resonance for the dimethyl groups at the xanthene scaffold in the ^{1}H NMR spectrum of the reaction mixture, from which **4′** was crystallized, suggesting a σ mirror plane along the xanthene plane of the product. DOSY experiments confirmed the presence of monomeric **4** in solution (see Supporting Information), and thus, a similar structure in solution as found for **3** is proposed.

Another common feature of both structures is that each aluminum and phosphorus atom is tetracoordinated, which raised the question whether the compounds show reactivity toward small molecules as the electrophilicity of the alane and the nucleophilicity of the phosphine appear quenched. Similar structures to **3** which also exhibit P–Al–X–Al structural motifs (with X = H) have been investigated by Uhl et al.,[4b] however, their reactivity toward substrates has not been reported.[9] To test whether **3** and **4**, respectively, can act as FLP, i.e. whether the Me_2AlCl unit in **3** is bound weakly enough to act as a replaceable space holder, solutions of **3** and **4** in toluene-d_8 were treated with an excess of THF, since the THF ring-opening reaction on a xanthene linked Al/P FLP has proved possible in our previous work.[6] In the ^{31}P NMR spectra recorded after both reactions a single new resonance was found at a chemical shift of $\delta = -18.8$ ppm (for **3**) and $\delta = -16.8$ ppm (for **4**), consistent with the coordination of a THF molecule to the xanthene-bound aluminum center. Heating the reaction mixtures to 80 °C for three days resulted in complete transformation of the intermediates to the THF ring-opened products resonating at $\delta = 26.5$ ppm (^{H}Xant(PPh$_2$(CH$_2$)$_4$O(AlMe$_2$Cl)AlMeCl), **5**, originating from **3**) and $\delta = 27.0$ ppm (^{tBu}Xant(PPh$_2$(CH$_2$)$_4$O(AlMe$_2$Cl)AlMeCl), **6**, originating from **4**), respectively, in the ^{31}P NMR spectra (Scheme 4). In both ^{1}H NMR spectra two resonances with an integral of three each can be observed belonging to the Me_2C unit in the xanthene backbone, which indicates an asymmetric structure of the products. Furthermore, the ^{1}H NMR spectra show that in contrast to the ring-opened compounds reported earlier, **5** and **6** feature a second alane moiety coordinating to the oxygen atom of the 4-oxybutyl bridge. For product **6** this was confirmed by single crystal X-ray diffraction (Figure 2).

Next, we addressed the question whether the FLPs **3** and **4** are also reactive toward a less donating and more inert

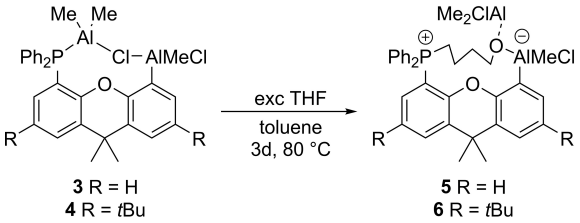

3 R = H
4 R = *t*Bu

5 R = H
6 R = *t*Bu

Scheme 4. THF cleavage by the FLPs **3** and **4** to give the betainic compounds **5** and **6**.

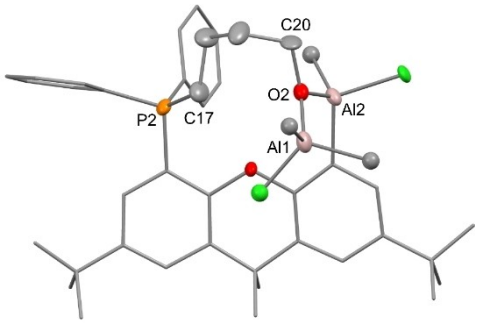

Figure 2. Molecular structure of **6** as determined by X-ray diffraction analysis. H atoms omitted for clarity; thermal ellipsoids drawn at the 50% probability level. Selected bond lengths (Å) and angles (°): P2-C17 1.798(2), Al1-O2 1.879(2), Al2-O2 1.846(2), O2-C20 1.467(3), Al1-O2-Al2 119.74(8), C20-O2-Al1 121.4(1), C20-O2-Al2 114.2(1).

substrate like CO_2. Therefore, a degassed solution of **3** and **4**, respectively, in toluene was treated with 2 bar $^{13}CO_2$ (Scheme 5). After 30 minutes at room temperature reaction control by ^{31}P NMR spectroscopy indicated full conversion of the starting compound to a product exhibiting a downfield-shifted broad doublet in both cases. The chemical shifts of $\delta = 12$ ppm (for **3**) and $\delta = 14$ ppm (for **4**) are in line with the chemical shifts of other reported CO_2 adducts of P/Al-based FLPs.[4a,5a,10] When the excess pressure of $^{13}CO_2$ was released, the rise of bubbles from the solution indicated a reversible process, which was confirmed after evaporating and redissolving the residues: ^{31}P NMR spectra revealed that the substrates **3** and **4**, respectively, were fully recovered. However, under CO_2 overpressure the product of the reaction of **3** with CO_2 could be crystallized from a supersaturated solution over time, giving single crystals of ^{H}Xant(PPh$_2$CO$_2$(AlMe$_2$Cl)AlMeCl), **7**·toluene, with sufficient stability and suitable quality for X-ray diffraction analysis.

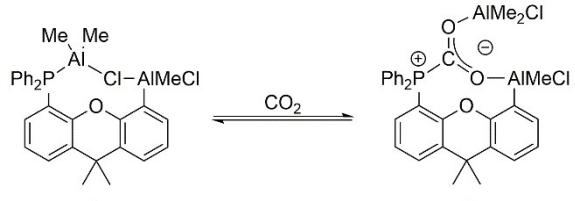

3 **7**

Scheme 5. Reversible capture of CO_2 by **3** forming **7**.

The solid state structure of **7** reveals the anticipated activation of CO_2 at the binding site spanned by the xanthene-bound alane and phosphine functions (Figure 3). While the phosphine expectedly binds to the carbon atom and the xanthene-bound aluminum atom to one of the oxygen atoms, the second oxygen atom coordinates to the additional dimethylaluminum chloride unit. This causes the two C–O bonds to be lengthened to a similar extent ($d_{C14\text{-}O3} = 1.249(2)$ Å vs. $d_{C14\text{-}O2} = 1.241(1)$ Å) as the formal negative charge is delocalized over the C(OAl)$_2$ moiety, comparable to the CO_2 adduct of the intermolecular Mes$_3$P/AlX$_3$ (X = Cl, Br) FLP by Stephan and coworkers.[10a] The O–C–O angle is 128.35(10)°; the sum of angles around the carbon atom is 360°, rendering the P–CO_2 unit trigonal planar.

We were now interested whether the equilibrium of the CO_2 capture can be shifted toward CO_2 fixation by increasing the Lewis acidity of the aluminum acceptor sites. Therefore, we also tested the precursors trimethylaluminum, methylaluminum dichloride and aluminum trichloride regarding their suitability for the aluminum-tin exchange reaction in contact with **1**. We found that the tendency of the alanes with the general formula Me$_x$AlCl$_{3-x}$ (x = 0–3) to react with **1** (0.5 equiv.) correlates with their Lewis acidity, i.e. while trimethylaluminum behaves inert even during several days at 100 °C, dimethylaluminum chloride (see above) and methylaluminum dichloride react selectively and are fully consumed after two days / one hour at room temperature, respectively; aluminum trichloride shows a highly unselective reactivity even at low temperatures. The product of the reaction of **1** with two equivalents MeAlCl$_2$ ^{H}Xant(PPh$_2$–AlMeCl$_2$–AlCl$_2$), **8**, is formed by elimination of Me$_4$Sn as indicated by ^{1}H NMR spectroscopy, and the chemical shift of $\delta = -19.1$ ppm in the ^{31}P NMR spectrum suggests an analogous structure as found for **3** (Scheme 6). Like **3** and **4**, compound **8** is highly sensitive toward moisture and oxygen and degrades at room temperature.

To attach a highly Lewis acidic diarylaluminum site on the xanthene-backbone, the reactivity of **1** toward MeAl(C$_6$F$_5$)$_2$ was

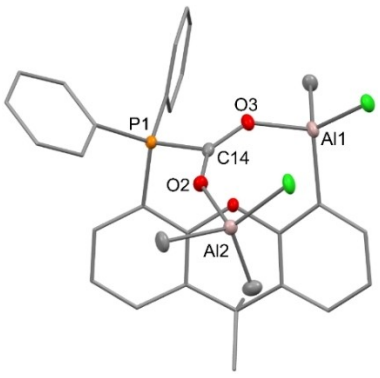

Figure 3. Molecular structure of **7**·toluene as determined by X-ray diffraction analysis. H atoms and co-crystallized solvent omitted for clarity; thermal ellipsoids drawn at the 50% probability level. Selected bond lengths (Å) and angles (°): P1-C14 1.883(1), Al1-O3 1.865(1), Al2-O2 1.8837(9), C14-O2 1.241(1), C14-O3 1.249(2), O2-C14-O3 128.3(1), P1-C14-O2 111.95(8), P1-C14-O3 119.71(8).

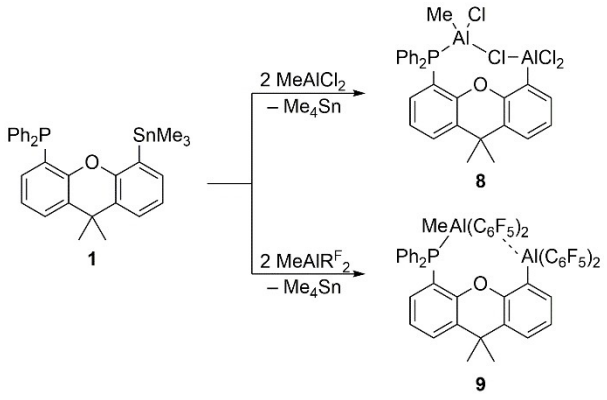

Scheme 6. Synthetic routes to more Lewis acidic xanthene-bound aluminum acceptor sites with chlorido (**8**) or pentafluorophenyl (**9**) substituents.

tested. Since the $MeAl(C_6F_5)_2$ bears two different Al–C bonds (Al–C(sp^3) and Al–C(sp^2)) that in principle can be transferred to the trimethyltin group producing either Me_4Sn or $Me_3Sn(C_6F_5)$, two different reaction courses were conceivable, with the one leading to $Al(C_6F_5)_2$ sites obviously being the more desirable.

Analogous to the aforementioned syntheses, two equivalents of freshly prepared $MeAl(C_6F_5)_2$ were required to achieve full conversion of the precursor **1**. After one hour at room temperature the ^{1}H NMR spectrum of the reaction mixture in toluene-d_8 showed both the formation of Me_4Sn ($\delta = 0.00$ ppm) and $Me_3Sn(C_6F_5)$ ($\delta = 0.21$ ppm) with an integral ratio of 4:1 (i.e. a $Me_4Sn/Me_3Sn(C_6F_5)$ ratio of 3:1), suggesting a notable preference of C(sp^3)-Al/Sn–C over C(sp^2)-Al/Sn–C metathesis. The presence of $Me_3Sn(C_6F_5)$ could be substantiated, as after evaporating and dissolving the mixture in $CDCl_3$ the ^{1}H NMR and ^{19}F NMR spectra showed the resonances reported for $Me_3Sn(C_6F_5)$.[11] The ^{19}F NMR spectrum of the reaction mixture exhibits four signal sets belonging to pentafluorophenyl groups, in line with a mixture of products containing C_6F_5 units. In the ^{31}P NMR spectrum two prominent resonances with chemical shifts of $\delta = -7.7$ and -9.0 ppm (integral ratio of roughly 1:2) were found, indicating full consumption of the precursor **1** ($\delta = -19.6$ ppm) and the occurrence of two main xanthene-based products. Altogether, these spectroscopic findings may be rationalized as follows: The observation of Me_4Sn in the ^{1}H NMR spectrum suggests the successful attachment of the $Al(C_6F_5)_2$ unit to the xanthene backbone, while the occurrence of $Me_3Sn(C_6F_5)$ is likely due to the introduction of a $Al(C_6F_5)Me$ unit to the linker scaffold. In both cases, the binding of the second equivalent of $MeAl(C_6F_5)_2$ is expected, so that the reaction mixture likely contains ^{H}Xant(PPh_2–$AlMe(C_6F_5)_2$-$Al(C_6F_5)Me$) as well as the desired product ^{H}Xant(PPh_2-$AlMe(C_6F_5)_2$–$Al(C_6F_5)_2$), **9** (Scheme 6), in addition to the accompanying tin compounds. Attempts to separate this complicated mixture and further characterize the products of interest failed.

Surprisingly, when an excess of THF is added to the reaction mixture in toluene-d_8, the ^{31}P NMR spectrum exhibits a sharp and intense signal at $\delta = -20.6$ ppm that accounts for $>90\%$ of P-based products according to ^{31}P NMR spectroscopy. This observation leads to the conclusion that the species found in the abovementioned reaction mixture are part of an equilibrium, and through shifting of this equilibrium a uniform reaction with THF can be reached. The resonance found at $\delta = -20.6$ ppm was attributed to the reported intermediate ^{H}Xant(PPh_2)($Al(C_6F_5)_2$(THF)) and this assignment was further substantiated through the analytical data of the product of the following ring-opening reaction, matching the ones reported for ^{H}Xant($PPh_2(CH_2)_4OAl(C_6F_5)_2$), **10** (Scheme 7).[6] In contrast to **6**, the second equivalent of $MeAl(C_6F_5)_2$ does not coordinate to the oxygen atom of the 4-oxybutyl bridge (see above) in **10**, probably due to steric hindrance, and is washed away during the work-up procedure.

The reactivity of the two freshly synthesized FLPs **8** and **9** toward CO_2 was investigated using the same conditions as for **3**. Solutions of **8** and **9**, respectively, in toluene-d_8 readily reacted when exposed to 2 bar CO_2 as indicated by their ^{31}P NMR spectra (Scheme 8). In case of **8**, the new signal, attributed to the product ^{H}Xant($PPh_2CO_2(AlMeCl_2)AlCl_2$), **11**, is downfield shifted ($\delta = 15$ ppm) and very broad, similar to the observations made for **7**. After the reaction of **9** a prominent new broad resonance with a chemical shift of $\delta = 10.6$ ppm appeared. It is noteworthy that - as in case of the THF reactions - the original two resonances ($\delta = -7.7$ and -9.0 ppm) found for the reaction mixture after the synthesis of **9**, vanish after exposure to CO_2 and the new signal assigned to the product ^{H}Xant(PPh_2CO_2(Al-$(C_6F_5)_2Me)Al(C_6F_5)_2$), **12**, at $\delta = 10.6$ ppm accounts for the major share of resonating phosphorus nuclei.

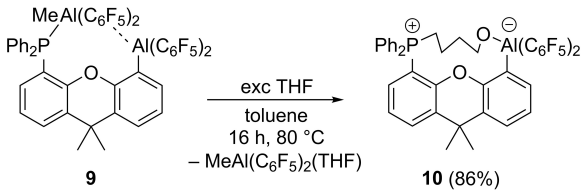

Scheme 7. Reactivity of **9** toward THF forming reported compound **10**.

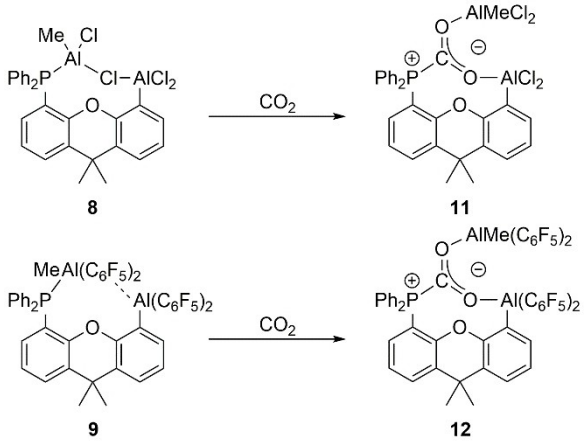

Scheme 8. Irreversible capture of CO_2 by **8** and **9**, respectively.

^{31}P NMR spectroscopic investigations revealed that evaporation of the solutions of **11** and **12** did not lead to the release of CO_2. Thus, as anticipated, the attachment of the electron withdrawing chloride (for **11**) and pentafluorophenyl (for **12**) substituents, which enhance the Lewis acidity of the aluminum acceptor sites, shifts the equilibrium of the CO_2 capture reaction strongly to the right side, so that, unlike in case of **3** and **4**, they are not reversible.

A supersaturated solution of **11**, from which single crystals slowly formed, was prepared by treating a concentrated solution of **8** with CO_2. Single crystals of **12** were grown by vapor diffusion of *n*-hexane into the reaction mixture of **12** in toluene. The solid state structures determined by X-ray diffraction analysis display the same connectivity as the structure of **7**·toluene, i.e. the CO_2 molecule is bound between the phosphine and alane moiety attached to the xanthene scaffold and the additional second equivalent of the applied organoaluminum reagent (Figure 4).

The CO_2 molecule is clearly activated as its C–O bonds are lengthened in both systems **11** and **12** compared to free gaseous CO_2 ($d_{C\text{-}O}$ = 1.1632 Å). Both C–O bonds are stretched to a similar extent and the P–CO_2 unit shows a trigonal planar structure, arguing for a delocalization of the negative charge over the C(OAl)$_2$ moiety. However, the structural parameters of **11** and **12** do not differ significantly from the ones exhibited by **7**, and there is no distinctive feature with regards to the CO_2 binding that would explain the irreversibility of CO_2 binding in case of **11** and **12**.

To fathom the difference in reversibility, quantum chemical calculations using density functional theory (DFT) were performed. Before addressing the calculated thermochemical and mechanistic data for the reaction of the FLPs **3**, **8**, and **9** with CO_2 in solution in detail, a closer look is taken at the computed (gas phase) binding energies ΔE_{bnd} of CO_2 in the corresponding reaction products **7**, **11**, and **12**, as they naturally constitute an essential factor of the reversibility or irreversibility of CO_2 capture. As can be seen from Table 1, ΔE_{bnd} of CO_2 in **7** and **11** is comparable in magnitude (−27 and −36 kJ mol^{-1}), although the difference of about 9 kJ mol^{-1} is a clear sign of the effect of the stronger Lewis acidic sites in **11** compared to **7**. In contrast to this notable but relatively small difference, a pronounced stability increase (by 73 kJ mol^{-1} relative to **11**) in binding energy is seen for the Al(C$_6$F$_5$)$_2$ system **12**.

To obtain more fundamental insights into these numbers, the intrinsic bonding situation was analyzed in detail based on EDA-NOCV calculations, and the results are also summarized in Table 1.

As expected, the orbital term ΔE_{orb} in this type of adducts is dominated by three main orbital interactions (about 84–85%), which comprise the P–CO_2 coordination covalent bond between the Lewis basic phosphorus atom and the activated CO_2 carbon atom, and two (CO)O–Al coordination covalent bonds resulting from interaction of the oxygen atoms with the aluminum centers. Plots of the corresponding deformation densities $\Delta\rho$ are depicted in Figure 5 for compound **7** as an example. By far the largest contribution to ΔE_{orb}, about 67% in all cases, stems from to the P–CO_2 interaction, while each of the (CO)O–Al interactions contribute about 8–10%. This result agrees well with the calculated Wiberg bond indices (WBIs), which indicate a considerably higher covalent character for the P–CO_2 bonds. The covalency of these bonds and, in contrast, ionicity of the (CO)O–Al interactions is also clearly reflected in the corresponding differences in the calculated NPA charges for the involved atoms (Table S1 in the Supporting Information). As can be seen from Table 1, the relative contributions for ΔE_{orb} stay almost constant across all adducts. However, the absolute values are notably larger for **11** compared to **7**, resulting in a larger orbital contribution term for the former. In contrast, the presence of pentafluorophenyl substituted aluminum centers in **12** does not result in a further enhancement of all the pairwise

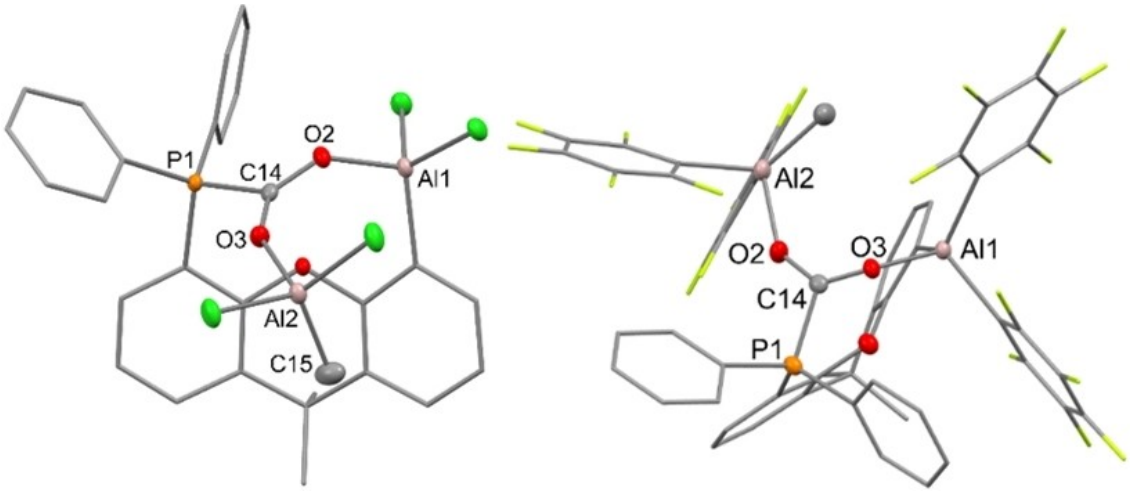

Figure 4. Molecular structures of **11**·toluene (left) and **12** (top down view, right) as determined by X-ray diffraction analysis. H atoms and co-crystallized solvent omitted for clarity; thermal ellipsoids drawn at the 50% probability level. Note, that in **11** the methyl group of C15 is disordered with a chloride. Selected bond lengths (Å) and angles (°): (for **11**) P1-C14 1.884(2), Al1-O2 1.840(1), Al2-O3 1.853(1), C14-O3 1.243(2), C14-O2 1.252(2), O2-C14-O3 127.3(1); (for **12**) P1-C14 1.882(2), Al1-O3 1.860(1), Al2-O2 1.898(1), C14-O2 1.239(2), C14-O3 1.251(2), O2-C14-O3 128.3(2).

Table 1. Results of EDA-NOCV analyses for the FLP:CO_2 bonding interactions in compounds **7**, **11**, and **12**, as well as Wiberg bond indices (WBIs) for selected bonds and NPA charges (q) for the CO_2 fragment. Energy values (in kJ mol^{-1}) were computed at the BP86-D3(BJ)/TZ2P level of theory.[a]

compound	ΔE_{bnd}[b]	ΔE_{prep}(FLP)	$\Delta E_{prep}(CO_2)$	ΔE_{prep}(total)	ΔE_{int}	WBI[c,d] P–C(O_2)	Al–O(CO)	q(CO_2)[c]
7	-27	237	216	454	−481	0.775	0.260	−0.77
11	−36	255	208	463	−499	0.786	0.259	−0.79
12	−109	192	207	399	−508	0.782	0.261	−0.78
	contributions to ΔE_{int}[a]							
	ΔV_{elstat}[e]	ΔE_{Pauli}	ΔE_{steric}[f]	ΔE_{orb}[e]	ΔE_{disp}[e]			
7	−891 (43.3%)	1575	684	−1103 (53.6%)	−62 (3.0%)			
11	−950 (43.6%)	1680	730	−1165 (53.4%)	−65 (3.0%)			
12	−922 (42.8%)	1645	722	−1155 (53.7%)	−75 (3.5%)			
	contributions to ΔE_{orb}[g]							
	$\Delta E(\rho_1)$	$\Delta E(\rho_2)$	$\Delta E(\rho_3)$	$\Delta E(\rho_{residual})$				
7	−741 (67.2%)	−96 (8.7%)	−88 (8.0%)	−178 (16.1%)				
11	−781 (67.1%)	−108 (9.3%)	−98 (8.4%)	−178 (15.3%)				
12	−777 (67.3%)	−112 (9.7%)	−92 (8.0%)	−175 (15.1%)				

[a] Energy-decomposition analyses with natural orbitals for chemical valence (EDA-NOCV) at MARIJ-BP86-D3(BJ)/def2-TZVP/COSMO(toluene) optimized structures. [b] Calculated reaction energy (BP86-D3(BJ)/TZ2P) for the activation of CO_2 by the FLPs **3**, **8**, **9**: FLP + CO_2→FLP-CO_2. [c] Wiberg bond indices and natural charges computed at BP86/def2-TZVP level. [d] The Wiberg bond indices for the two Al–O(CO) bonds in the molecules are given as average value. [e] The values in parentheses give the percentage contribution to the total attractive interactions. [f] $\Delta E_{steric} = \Delta V_{elstat} + \Delta E_{Pauli}$. [g] The values in parentheses give the percentage contribution to the total orbital interaction ΔE_{Orb}.

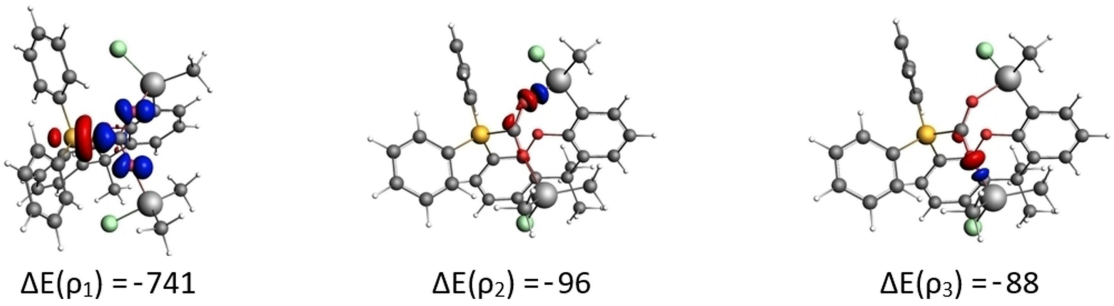

Figure 5. Contour plots (isosurface value ±0.005 a.u.) of NOCV deformation densities Δρ and associated orbital stabilization energies (ΔE(ρ), in kJ mol^{-1}) of the three dominant pairwise FLP:CO_2 orbital interactions in **7** (BP86-D3(BJ)/TZ2P). Electronic charge flow is from red to blue.

interactions compared to the situation in **11**. Instead, an overall slight decrease of ΔE_{orb} can be noted.

The calculated total interaction energies ΔE_{int} for the investigated products of CO_2 activation span a rather narrow range of 27 kJ mol^{-1}. As anticipated, a successive increase of ΔE_{int} for the CO_2 and FLP fragment interactions is observed in the order **7** (−481 kJ mol^{-1}) < **11** (−499 kJ mol^{-1}) < **12** (−508 kJ mol^{-1}). This appears to be fully consistent with an enhanced FLP:CO_2 bonding as consequence of a paralleling increase in Lewis acidity of the organoaluminum acceptor sites. Partial substitution of methyl with chloride in the FLP, i.e., transition from **7** to **11**, raises ΔE_{int} by about 18 kJ mol^{-1}. However, substitution with the even stronger electronegative C_6F_5 groups in **12** enhances the interaction by only 9 kJ mol^{-1} relative to **11**. A breakdown of the interaction energies into their individual contributions shows that almost all terms, attractive and repulsive, are significantly larger for the $AlCl_2$-FLP **11** compared to **7**. The increase in orbital interaction ΔE_{orb} is consistent with a higher degree of covalent bonding in **11**, which is partly compensated by the slightly larger repulsive sterics term ΔE_{steric} ($= \Delta V_{elstat} + \Delta E_{Pauli}$). Owing to the similarity in structure and composition, the dispersive interaction contribution is only slightly larger in **11** (about 3 kJ mol^{-1}). In contrast, compared to **11** the repulsive and most of the attractive terms are smaller again in the C_6F_5-substituted **12**. The notable exception is the ΔE_{disp}. contribution, which is by 10 kJ mol^{-1} larger. The overall increase of ΔE_{int} in **12** thus essentially originates from enhanced dispersive interactions, not as a consequence of stronger orbital and weaker sterics contributions. We note also that electrostatic contributions remain relatively similar for all three systems, consistent with the similar NPA charges of the CO_2 fragment (Table 1).

While the total interaction energies match the trend of the computed binding energies, the differences in ΔE_{int} and ΔE_{bnd} show that the former remarkably accounts for only about 12% ($\Delta\Delta E_{int} = 9$ kJ mol^{-1}) of the observed increase in stability ($\Delta\Delta E_{bnd} = 73$ kJ mol^{-1}) when comparing **11** and **12**. The origin of the particularly large binding energy of CO_2 in **12** is thus clearly a result of the significantly smaller reorganization energy ΔE_{prep} in this case, that is, the necessary structural changes in the reactant FLP **9** to accommodate a CO_2 molecule.

This smaller reorganization energy can be traced back to a considerably altered bonding situation regarding the Lewis acidic centers in the reactant structure of **9** (Figure 6) compared

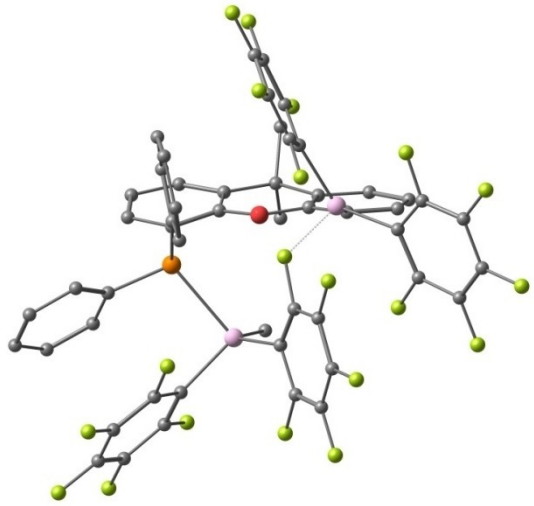

Figure 6. Calculated molecular structure of **9** (MARIJ-BP86-D3(BJ)/def2-TZVP/COSMO(toluene)). Hydrogen atoms have been omitted for clarity.

to **3** (Figure 1) and **8**. While a chlorine atom acts as a strong linker between the aluminum sites in the latter compounds, inspection of the most favorable computed structure for **9** (Figure 6) reveals that neither a methyl nor a C_6F_5 group (symmetrically or asymmetrically) bridges the centers via a shared carbon atom, as might be expected. Instead, the xanthene-bound aluminum acceptor exhibits an Al···F interaction with one of the pentafluorophenyl rings of the phosphorus-coordinated $MeAl(C_6F_5)_2$ unit, showing a comparably long aluminum-fluorine distance of 2.022 Å. At the same time, the Al–P distance in **9** is noticeably elongated (2.525 Å) compared to **3** and **8** (2.474 and 2.439 Å). The same holds true for the Al···Al spacing, which is naturally rather similar for **3** and **8** (2.365 and 2.330 Å), but significantly enlarged in case of **9** (4.646 Å). Due to the smaller size of the substituents at Al in **3** and **8**, the second AlR_3 group can occupy a position much closer to the P···Al axis of the FLP core in these compounds. Hence, despite the higher Lewis acidity the computed parameters seem to indicate a weaker bound central $MeAl(C_6F_5)_2$ unit, adopting a comparably detached position. This in turn would explain the relatively small reorganization energy necessary to enable activation of CO_2.

As shown experimentally, compounds **3** and **8** are both able to activate CO_2, but also constitute borderline cases for a reversible (**3**) or irreversible (**8**) binding of CO_2. In view of the comparably small difference in ΔE_{bnd} for **7** and **11** discussed above, the origin of reversible/irreversible CO_2 binding is apparently rooted in the corresponding barrier height for activation. To elucidate the basic kinetics behind this difference in reversibility, further DFT calculations at a more sophisticated level (see Computational Details) have been carried out to obtain the free energy profiles in toluene solution for the first steps of carbon dioxide activation by **3** and **8**. The calculations reveal that a direct insertion of CO_2 into the Al–P bond exhibits a free energy barrier for both compounds which is too high to be overcome at room temperature ($\Delta_rG^{\ddagger} = 146\ kJ\,mol^{-1}$ (**3**)/ $166\ kJ\,mol^{-1}$ (**8**); TS_3 in Scheme S1 in the Supporting Information). Instead, the initial reaction does not necessarily involve CO_2 at all. As shown in Scheme 9, the first process step is likely a dissociation of the central aluminum unit from the Lewis basic diphenylphosphine site to form an intermediate (Int_1), which features a classical chlorine-bridged dimeric structural motif of the Al centers. The corresponding transition states are much lower in free energy as compared to those of the direct CO_2 insertion (TS_1; $\Delta_rG^{\ddagger} = 54\ kJ\,mol^{-1}$ (**3**)/$76\ kJ\,mol^{-1}$ (**8**)), rendering this process feasible at room temperature. Presumably, the energy loss due to the breaking of the P–Al bond is partly compensated by the concomitant formation of the second Al–Cl bridge, thus lowering the barrier. This opens up a cavity

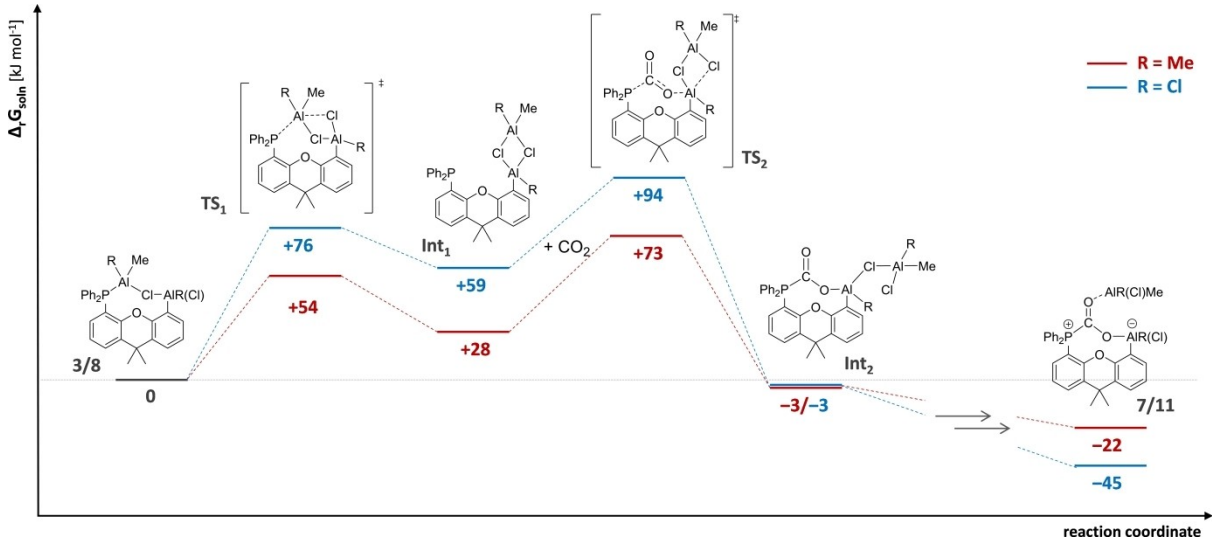

Scheme 9. Free energy profile for the activation of CO_2 with compounds **3** (red lines) and **8** (blue lines), respectively. All reaction and activation free energies (Δ_rG_{soln}, in $kJ\,mol^{-1}$, 298.15 K, 0.1 MPa) in toluene solution are given relative to the separate reactants (MARIJ-ωB97M-V/def2-TZVPP/COSMO-RS(toluene)).

where CO_2 can more easily interact with both the Lewis acidic and the (now activated) basic site. To some extent this process shares similarities with the mechanism for CO_2 activation found for other (intermolecular) P/Al-based FLPs in coordinating solvents.[12] The FLPs in this study however, by construction, exhibit an intramolecular coordination environment by means of the second AlR_3 unit that helps to facilitate the transformation, and thus does not have to rely on an external coordinating solvent. The rate-determining step on the profile is the second transition state TS_2, in which the actual CO_2 activation takes place, and which leads to the formation of intermediate Int_2. The latter can subsequently rearrange into the respective final product **7** ($\Delta_rG = -22\ kJ\,mol^{-1}$) or **11** ($\Delta_rG = -45\ kJ\,mol^{-1}$). Similar to TS_1, FLP **8** exhibits a barrier for CO_2 activation which is about 20 $kJ\,mol^{-1}$ higher in free energy than in case of **3** (TS_2; $\Delta_rG^{\neq} = 73\ kJ\,mol^{-1}$ (**3**) / 94 $kJ\,mol^{-1}$ (**8**)). The general observation of higher barriers reflects the stronger Lewis acidic sites in FLP **8**, which makes the cleavage of P–Al and Al–Cl bonds energetically more demanding. While the activation free energy that is required for TS_2 for both compounds is still much lower compared to a direct insertion, the transition state of **8** is likely energetically at the brink of a feasible room temperature process. Consequently, the substantial gain in thermodynamic stability upon formation of product **11** ($\Delta_rG = -45\ kJ\,mol^{-1}$) renders the reverse reaction impossible under these conditions. In contrast, and in line with the experimental findings, the reverse reaction is energetically still possible for product **7**, as its required total activation free energy of $\Delta_rG^{\neq} = 95\ kJ\,mol^{-1}$ is similar in magnitude to TS_2 in the forward process of **8**.

Conclusion

In conclusion, an aluminum-tin exchange has been successfully utilized for the synthesis of an intramolecular P/Al-based FLP on a xanthene scaffold. The large spatial separation between the donor and acceptor sites is unprecedented in the chemistry of unimolecular aluminum FLPs. Even though a second organoaluminum precursor molecule is incorporated in the reaction pocket, the compounds show reactivity toward small molecules such as THF and CO_2. The reversibility of the CO_2 capture at room temperature is dependent on the Lewis acidity of the aluminum sites, tuned by their substituents, and in turn by the thermodynamic stability of the products and the associated reaction barriers. Thermodynamically, the CO_2 adduct **11** is significantly more stable than **7** and the origin for irreversibility is the much larger barrier for the back reaction. In case of **12** there is an additional effect that strongly increases the energy for the binding of CO_2 as compared to **11**, namely the significantly smaller reorganization energy due to the fact that the structure of **9** accommodates a CO_2 molecule with far less changes as compared to **8**.

Our future efforts will focus on the synthesis of an intramolecular FLP comprising an aluminum acceptor and a phosphine donor site in a 1:1 stoichiometry, which would allow for further functionalization of the Al-center by different substituents.

Experimental Section

Crystallographic data

Deposition Number(s) 2150565, 2150566, 2150567, 2150568, 2150569, 2150570, 2150571 and 2150572 contain(s) the supplementary crystallographic data for this paper. These data are provided free of charge by the joint Cambridge Crystallographic Data Centre and Fachinformationszentrum Karlsruhe Access Structures service.

Acknowledgements

We thank Dr. André Dallmann for the DOSY measurements. Funded by the Deutsche Forschungsgemeinschaft (DFG, German Research Foundation) – Project-ID 387284271 – SFB 1349. Open Access funding enabled and organized by Projekt DEAL.

Conflict of Interest

The authors declare no conflict of interest.

Data Availability Statement

The data that support the findings of this study are available in the supplementary material of this article.

Keywords: aluminum · carbon dioxide · FLP · phosphane · unimolecular

[1] a) G. Kehr, S. Schwendemann, G. Erker, in *Frustrated Lewis Pairs I: Uncovering and Understanding* (Eds.: G. Erker, D. W. Stephan), Springer Berlin Heidelberg, Berlin, Heidelberg, **2013**, pp. 45–83; b) F. A. Tsao, D. W. Stephan, *Dalton Trans.* **2015**, *44*, 71–74; c) K. Chernichenko, B. Kótai, I. Pápai, V. Zhivonitko, M. Nieger, M. Leskelä, T. Repo, *Angew. Chem. Int. Ed.* **2015**, *54*, 1749–1753; *Angew. Chem.* **2015**, *127*, 1769–1773; d) M.-A. Courtemanche, M.-A. Légaré, L. Maron, F.-G. Fontaine, *J. Am. Chem. Soc.* **2014**, *136*, 10708–10717; e) K. Chernichenko, Á. Madarász, I. Pápai, M. Nieger, M. Leskelä, T. Repo, *Nat. Chem.* **2013**, *5*, 718–723; f) M.-A. Légaré, M.-A. Courtemanche, É. Rochette, F.-G. Fontaine, *Science* **2015**, *349*, 513–516; g) J. L. Lavergne, A. Jayaraman, L. C. Misal Castro, É. Rochette, F.-G. Fontaine, *J. Am. Chem. Soc.* **2017**, *139*, 14714–14723; h) K. Chernichenko, M. Lindqvist, B. Kótai, M. Nieger, K. Sorochkina, I. Pápai, T. Repo, *J. Am. Chem. Soc.* **2016**, *138*, 4860–4868; i) M.-A. Courtemanche, A. P. Pulis, É. Rochette, M.-A. Légaré, D. W. Stephan, F.-G. Fontaine, *Chem. Commun.* **2015**, *51*, 9797–9800; j) D. H. A. Boom, E. J. J. de Boed, E. Nicolas, M. Nieger, A. W. Ehlers, A. R. Jupp, J. C. Slootweg, *Z. Anorg. Allg. Chem.* **2020**, *646*, 586–592.

[2] M.-A. Courtemanche, J. Larouche, M.-A. Légaré, W. Bi, L. Maron, F.-G. Fontaine, *Organometallics* **2013**, *32*, 6804–6811.

[3] Recently, a novel synthetic route to an ethylene bridged P/Al-FLP was reported. However, the C_2 bridge was eliminated when the FLP was exposed to common substrates applied in FLP chemistry: T. Yanagisawa, Y. Mizuhata, N. Tokitoh, *Chem. Eur. J.* **2021**, *27*, 11273–11278.

[4] a) C. Appelt, H. Westenberg, F. Bertini, A. W. Ehlers, J. C. Slootweg, K. Lammertsma, W. Uhl, *Angew. Chem. Int. Ed.* **2011**, *50*, 3925–3928; *Angew.*

Chem. **2011**, *123*, 4011–4014; b) W. Uhl, C. Appelt, J. Backs, H. Westenberg, A. Wollschläger, J. Tannert, *Organometallics* **2014**, *33*, 1212–1217; c) H. Klöcker, S. Roters, A. Hepp, W. Uhl, *Dalton Trans.* **2015**, *44*, 12670–12679; d) L. Keweloh, H. Klöcker, E.-U. Würthwein, W. Uhl, *Angew. Chem. Int. Ed.* **2016**, *55*, 3212–3215; *Angew. Chem.* **2016**, *128*, 3266–3269; e) D. Pleschka, M. Layh, F. Rogel, W. Uhl, *Philos. Trans. R. Soc. London Ser. A* **2017**, *375*, 20170011; f) L. Keweloh, N. Aders, A. Hepp, D. Pleschka, E.-U. Würthwein, W. Uhl, *Dalton Trans.* **2018**, *47*, 8402–8417; g) M. Tolzmann, L. Schürmann, A. Hepp, W. Uhl, M. Layh, *Eur. J. Inorg. Chem.* **2020**, *2020*, 4024–4036; h) T. Holtrichter-Rößmann, C. Rösener, J. Hellmann, W. Uhl, E.-U. Würthwein, R. Fröhlich, B. Wibbeling, *Organometallics* **2012**, *31*, 3272–3283.

[5] a) J. Boudreau, M.-A. Courtemanche, F.-G. Fontaine, *Chem. Commun.* **2011**, *47*, 11131–11133; b) H. H. Karsch, A. Appelt, F. H. Koehler, G. Mueller, *Organometallics* **1985**, *4*, 231–238; c) A. Bodach, N. Nöthling, M. Felderhoff, *Eur. J. Inorg. Chem.* **2021**, *2021*, 1240–1243; d) S. Chen, B. Li, X. Wang, Y. Huang, J. Li, H. Zhu, L. Zhao, G. Frenking, H. W. Roesky, *Chem. Eur. J.* **2017**, *23*, 13633–13637; e) Y. Chen, W. Jiang, B. Li, G. Fu, S. Chen, H. Zhu, *Dalton Trans.* **2019**, *48*, 9152–9160; f) C. Böker, M. Noltemeyer, H. Gornitzka, B. O. Kneisel, M. Teichert, R. Herbst-Irmer, A. Melier, *Main Group Met. Chem.* **1998**, *21*, 565–580; g) E. Hupf, E. Lork, S. Mebs, L. Chęcińska, J. Beckmann, *Organometallics* **2014**, *33*, 7247–7259; h) H. Schumann, S. Dechert, M. Hummert, K. C. H. Lange, S. Schutte, B. C. Wassermann, K. Köhler, J. Eichhorn, *Z. Anorg. Allg. Chem.* **2004**, *630*, 1196–1204; i) H. Schumann, B. C. Wassermann, S. Schutte, B. Heymer, S. Nickel, T. D. Seuß, S. Wernik, J. Demtschuk, F. Girgsdies, R. Weimann, *Z. Anorg. Allg. Chem.* **2000**, *626*, 2081–2095.

[6] P. Federmann, C. Herwig, F. Beckmann, B. Cula, C. Limberg, *Organometallics* **2021**, *40*, 4143–4149.

[7] a) M. Tschinkl, F. P. Gabbaï, R. E. Bachman, *Chem. Commun.* **1999**, *15*, 1367–1368; b) J. J. Eisch, K. Mackenzie, H. Windisch, C. Krüger, *Eur. J. Inorg. Chem.* **1999**, *1999*, 153–162.

[8] L. A. van der Veen, P. K. Keeven, P. C. J. Kamer, P. W. N. M. van Leeuwen, *Chem. Commun.* **2000**, *5*, 333–334.

[9] Note, that dimeric structures comparable to **4** react with CO_2 and isocyanates: S. Roters, C. Appelt, H. Westenberg, A. Hepp, J. C. Slootweg, K. Lammertsma, W. Uhl, *Dalton Trans.* **2012**, *41*, 9033–9045.

[10] a) G. Ménard, D. W. Stephan, *J. Am. Chem. Soc.* **2010**, *132*, 1796–1797; b) G. Ménard, T. M. Gilbert, J. A. Hatnean, A. Kraft, I. Krossing, D. W. Stephan, *Organometallics* **2013**, *32*, 4416.

[11] G. E. Rudebusch, L. N. Zakharov, S.-Y. Liu, *Angew. Chem. Int. Ed.* **2013**, *52*, 9316–9319; *Angew. Chem.* **2013**, *125*, 9486–9489.

[12] H. J. Kwon, H. W. Kim, Y. M. Rhee, *Chem. Eur. J.* **2011**, *17*, 6501–6507.

Manuscript received: February 8, 2022
Accepted manuscript online: February 25, 2022
Version of record online: March 22, 2022